iScience, Volume *23*

Supplemental Information

Mixed Selectivity in Macaque Medial Parietal Cortex during Eye-Hand Reaching

Stefano Diomedi, Francesco E. Vaccari, Matteo Filippini, Patrizia Fattori, and Claudio Galletti

SUPPLEMENTAL INFORMATION

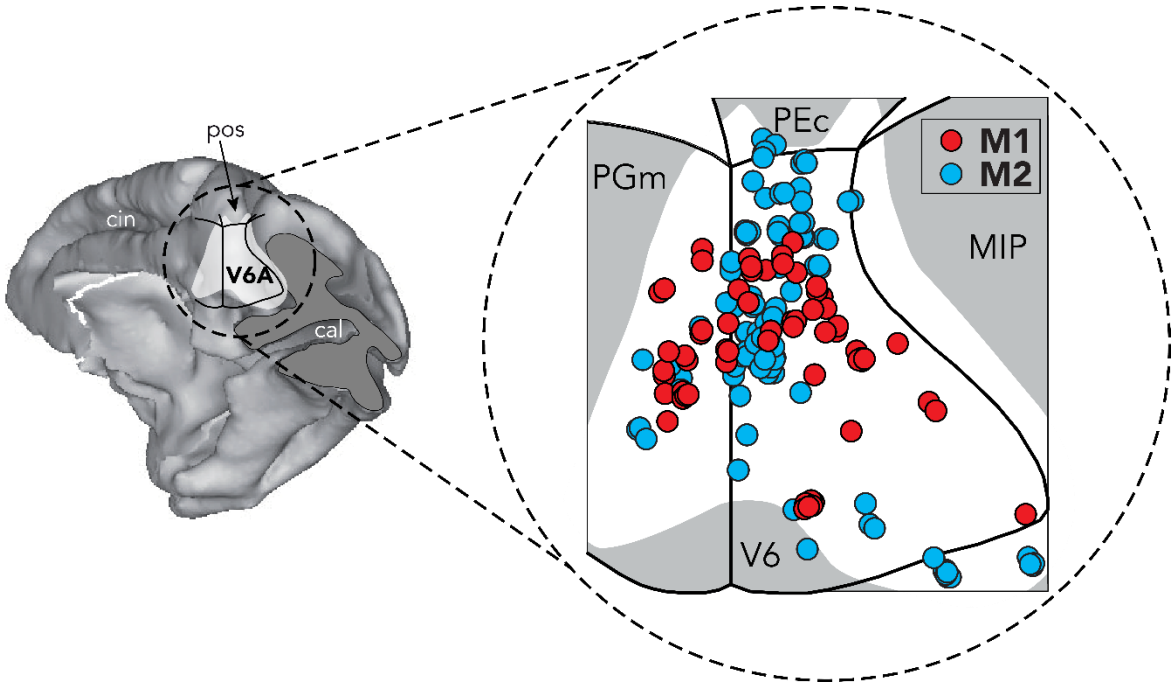

FIG. S1 Recording sites in the two animals, Related to Fig. 1.

On the left, posteromedial view of 3D-reconstructed macaque brain. The posterior part of the occipital lobe was cut off to visualize the entire extent of the anterior bank of parieto-occipital sulcus. Superimposed, a flattened map of the caudal part of the SPL. The level of the cut is shown in grey. On the right, the 2D map of caudal SPL with the locations of recorded neurons in area V6A for the 2 monkeys (red M1, blue M2). Abbreviations: cal, calcarine sulcus; pos, parieto-occipital sulcus; cin, cingulate sulcus.

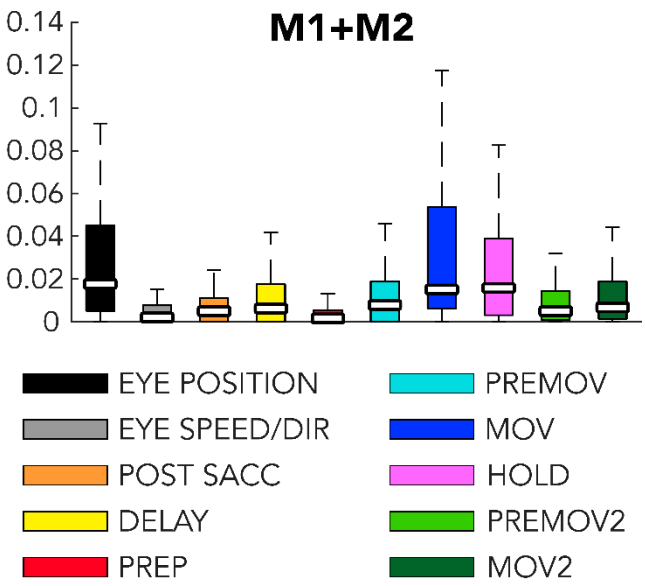

FIG. S2 Extrinsic regressors' influence across the population (two animals' data were pooled together, related to Fig. 3

Box plot of the w-values for each block of regressors across the population obtained merging data from the 2 animals. Other conventions as fig. 3A.

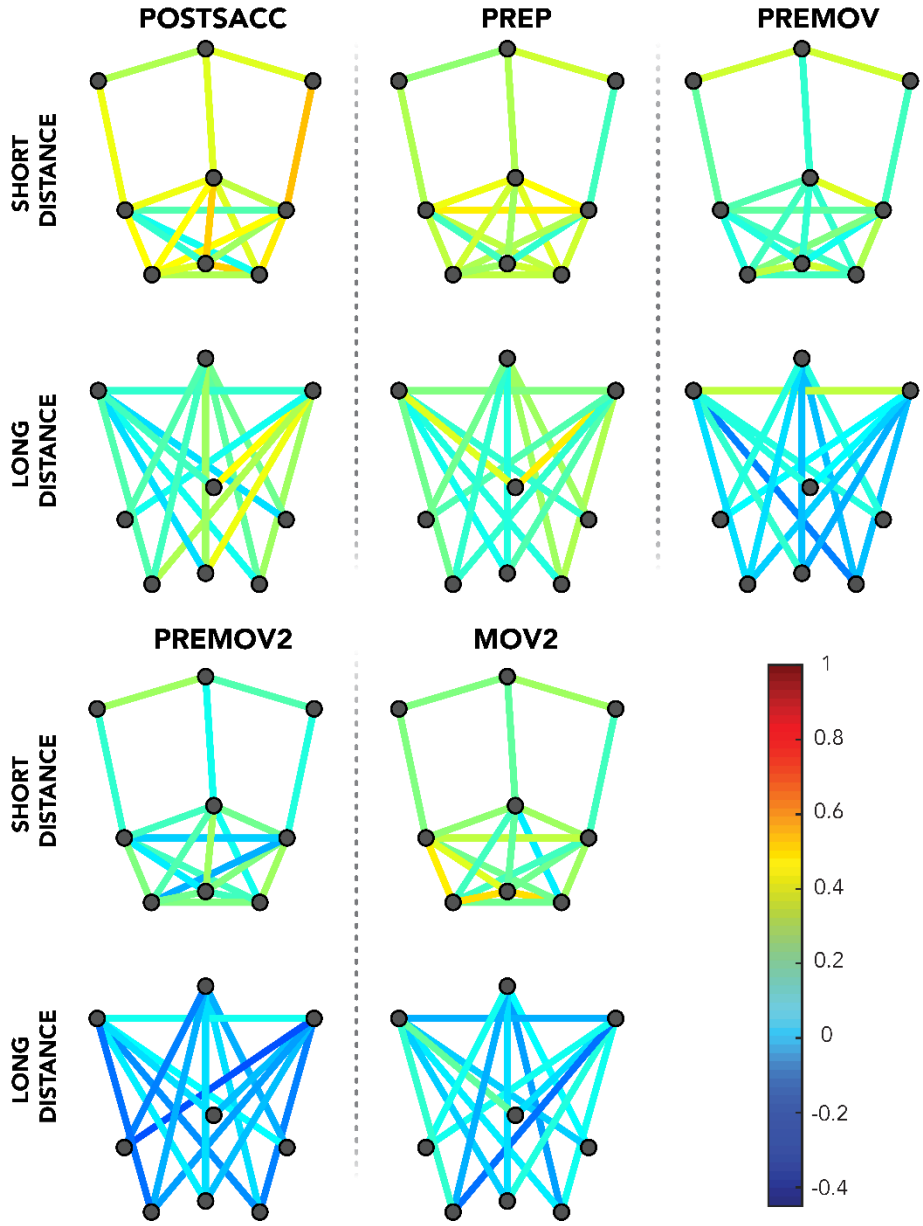

FIG. S3 Correlations between beta coefficients relative to different target positions across the population, related to Fig. 4

Panels are paired for short/long distances and columns are results for POSTSACC, PREP, PREMOV, PREMOV2, MOV2 epochs. Other conventions as fig. 4C.

	EYEPOS	EYESPEED	POSTSACC	DELAY	PREP	PREMOV	MOV	HOLD	PREMOV2	MOV2
M1	'0.018 [0.004 0.050]'	'0.003 [0.0005 0.009]'	'0.008 [0.0008 0.014]'	'0.006 [0 0.016]'	'0.0015 [0 0.007]'	'0.014 [0.001 0.030]'	'0.011 [0.003 0.033]'	'0.011 [0.003 0.032]'	'0.006 [0.001 0.017]'	'0.007 [0.0005 0.019]'
M2	'0.017 [0.005 0.044]'	'0.001 [0 0.007]'	'0.0003 [0 0.009]'	'0.007 [0 0.019]'	'0.001 [0 0.005]'	'0.005 [0 0.013]'	'0.030 [0.008 0.066]'	'0.019 [0.003 0.054]'	'0.004 [0.0005 0.012]'	'0.007 [0.002 0.016]'
M1 + M2	'0.018 [0.004 0.045]'	'0.002 [0 0.008]'	'0.004 [0 0.011]'	'0.005 [0 0.017]'	'0.001 [0 0.005]'	'0.007 [0 0.019]'	'0.015 [0.006 0.054]'	'0.015 [0.003 0.039]'	'0.005 [0.001 0.014]'	'0.007 [0.001 0.018]'

Table S1. 'Median [25-th percentile 75-th percentile]' of the w-values for the M1, M2, M1+M2 relative to every block of regressors, related to Fig. 3

Transparent methods

The current study consisted in an extended computational analysis of neural data reported previously (Breveglieri et al., 2014). Accordingly, the procedures described herein focus on analytical treatment of the data and provide only essential details of the behavioural and electrophysiological procedures. Full details of experimental methods are provided in our previous reports.

The study was performed in accordance with the guidelines of the EU Directives (86/609/EEC; 2010/63/EU) and the Italian national law (D.L. 116-92, D.L. 26-2014) on the use of animals in scientific research. Protocols were approved by the Animal-Welfare Body of the University of Bologna. During training and recording sessions, particular attention was paid to any behavioral and clinical sign of pain or distress.

Experimental Procedures

Two male macaque monkeys (Macaca fascicularis) weighting 4.4 kg (M1) and 3.8 kg (M2) were used. Single cell activity was extracellularly recorded from the anterior bank of the parieto-occipital sulcus (POs). The electrodes entered directly into the cortex of the exposed surface of the caudal aspect of superior parietal lobule or passed through the occipital pole and the POs to reach the anterior bank of the sulcus in the depth (inclination angle of electrodes was 28–30°posteriorly from the coronal plane). After passing through areas V1–V2 of the occipital lobe, the electrode reached the anterior bank of the POs at a variable depth (up to 8mm) according to the anteroposterior coordinate of penetration. Area V6A was initially recognized on functional grounds following the criteria described in (Galletti et al. 1999) and later confirmed based on the cytoarchitectonic criteria of (Luppino et al. 2005).

We performed multiple electrode penetrations using a five-channel multielectrode recording system (Thomas Recording GmbH, Giessen, Germany). The electrode signals were amplified (at a gain of 10,000) and filtered (bandpass between 0.5 and 5 kHz). Action potentials in each channel were

isolated with a waveform discriminator (Multi Spike Detector; Alpha Omega Engineering Nazareth, Israel) and were sampled at 100 kHz. Quality of single-unit isolation was determined by the homogeneity of spike wave forms and clear refractory periods in ISI histograms during spike-sorting. Only well-isolated units not changing across tasks were considered. The animal behaviour was controlled by custom-made software implemented in LabVIEW (National Instruments, Austin, TX) environment (Kutz et al. 2005). Eye position signals were sampled with two cameras (one for each eye) of an infrared oculometer system (ISCAN, Woburn, MA) at 100 Hz. The vergence angle was not recorded online, but it was reconstructed offline from the horizontal eye positions of the two eyes. A sort of control for vergence resulted from the presence of electronic windows (one for each eye, 4° × 4° each) that controlled the fronto-parallel gaze position, so that we could set an offset of the horizontal eye position signal for targets located in the same direction, but at different depths.

Behavioural Task

Electrophysiological signals were collected while the monkeys were performing an instructed-delay body-out reaching task (Fig. 1B-C). The targets were located in different positions in the 3-D space. During the task the animals were fixating a target that they would reach when instructed. Monkeys sat in a primate chair, with the head restrained, and faced a horizontal panel located at eye level. Nine light-emitting diodes (LEDs) mounted on the panel at different distances from the eyes were used as fixation and reaching targets (Fig. 1B, left). As shown in the right part of Fig. 1B, the target LEDs were arranged in three rows: one central, along the sagittal midline, and two laterals, at isoversion angles of −15° and +15°, respectively. Along each row, three LEDs were located at isovergent positions of 17.1°, 11.4°, and 6.9°, respectively. The two animals had the same interocular distance (3.0 cm), so we placed the isovergent rows at the same distance from the monkeys in both animals (nearest targets: 10 cm from monkey eyes; intermediate targets: 15 cm; far targets: 25 cm). The range of vergence angles was chosen to be within the limits of peripersonal space, so the monkeys were able to reach all target positions. The animals performed the task with the limb contralateral to the

recording site while maintaining steady fixation. The hand started the trial pushing a button (home button, 2.5 cm in diameter, Fig. 1B, C) placed outside the monkeys' visual field, 5 cm in front of its trunk. 1000 ms after home button pressing one of the 9 LEDs lit up green. The monkeys were required to fixate the fixation point while keeping the button pressed. The fixation point served as a cue concerning the direction of the arm movement to perform. However, the monkeys needed to withhold the instructed behaviour without performing any eye or arm reaching movement for 1700–2500 ms, till the change in colour of fixation LED (green to red). The colour change of fixation target was the go signal for the animal to release the home button and start an arm movement toward the target. The monkeys had 1 sec after the go signal to reach the target; otherwise, the trial was aborted. Then, monkeys pushed the target and held the hand on it for 800–1200 ms. The target offset cued the monkeys to release the LED and return to the home button, which ended the trial and allowed monkeys to receive reward. Notice that since target offset, the animals were allowed to break fixation. Only correctly executed trials were used in this analysis.

Poisson GLM and LASSO optimization

Generalized linear models (GLMs) are a flexible generalization of ordinary linear regression used for variables that have distribution other than Gaussian. In this sense, ordinary linear regressions can be seen as a specific type of GLM.

In premotor (Takahashi et al., 2017) and somato-motor (Goodman et al., 2019) (Hatsopoulos et al., 2007), for instance, GLMs (or ordinary linear regressions) provided interesting insights about the neural modulations for several kinematic parameters of the upper limb. In different contexts, also gaze position can be included in these models (Lehmann and Scherberger, 2013).

Poisson distribution is used for modelling the number of times that an event occurs in an interval of time. So, the behaviour of a neuron (i.e. variations of its spiking activity) can be modelled as a Poisson process (Fig. 1D) (Triplett and Goodhill, 2019; Pillow et al., 2008; Truccolo et al., 2005; Paninski et

al., 2004b; Dayan and Abbott, 2001). Thus, the probability of observing the spike count y from a neuron in a short period of time is:

$$P(y|\mu,\Delta) = \frac{e^{-\mu\Delta}\mu\Delta^{y}}{y!}$$

where μ represent the firing rate over unit time and Δ is the bin width.

GLM with Poisson distribution assumes that the varying firing rate at a specific time t can be represented as the exponential of the linear combination of the parameters called regressors (Fig. 1D), and so:

$$\mu_t = \exp(\beta_0 + \beta_1 X_{1,t} + \ldots + \beta_K X_{K,t})$$

where K is the number of regressors, $\{\beta_k\}_{k=1,\ldots K}$ are the regression coefficients, each$X_{k,1\ldots T}$ is a vector of regressors and β_0 is the constant of the model.

The regression coefficients are estimated through a procedure called Maximum Likelihood Estimation (MLE) that maximizes the log-likelihood (the logarithm of the likelihood, computationally easier to calculate), i.e. the probability, given a model, to observe a given spike train. The log-likelihood function for Poisson GLMs can be calculated as (Goodman et al., 2019):

$$\ell(y,\beta) = \log[L(y,\beta)] = \sum_{t=1}^{T} y_t \log(\mu_t) - \mu_t$$

We followed a procedure similar to the one recently adopted by Goodman and colleagues (2019). In a first phase of the fitting, we applied an optimization method called LASSO, which is used to avoid over-fitting and to select the more significant regressors because it shrinks the size of the regression coefficient and sets the unimportant ones to zero. For this aim, we added the LASSO penalty term to the log-likelihood and maximized the resulting function:

$$\hat{\beta}_{LASSO} = \mathrm{argmax}_{\beta}\left(\ell(y,\beta) - \lambda\sum_{k=1}^{K}|\beta_k|\right)$$

and where λ represents the strength of the LASSO shrinkage. After this, we applied the classic MLE regression with only the selected regressors to get not penalized β coefficients:

$$\hat{\beta}_{\mathrm{MLE}} = \mathrm{argmax}_{\beta}\ell(y, \beta)$$

in this way we estimate only coefficients related to significant regressors.

Data pre-processing

We aligned data on the release of home button, then we considered neural activity and eye tracks for all neurons for all trials from -3000 ms to +1720 ms. Cropping trials in this way allowed us to capture the last part of free epoch and the beginning of fixation for every trial; after the release of home button we captured the whole hold epoch and the returning of arm to the resting position for most of trials. We then binned spiking activity at 40 ms calculating the number of spikes in each bin. We chose this binning interval because we wanted to focus the influence of each regressor on cell activity expressed as its firing rate, rather than predict each spike precisely and direct the attention on spiking mechanics.

For each bin, we calculate the averaged gaze position along x and y coordinates for the two eyes (each 40 ms bin contains 4 points of the raw eye track sampled at 10 ms). We averaged x-position for the two eyes (R_x, L_x) and y-position for the two eyes (R_y, L_y), getting a couple of values that indicates for each bin real gaze direction (version and elevation).

$$VERSION = \frac{R_x + L_x}{2};\ ELEVATION = \frac{R_y + L_y}{2}$$

We also got horizontal vergence for each bin applying the formula:

$$\mathrm{VERGENCE} = L_x - R_x$$

Extrinsic regressors

As gaze modulations are not linear (Breveglieri et al., 2012; Galletti et al., 1995), in order to capture the responses' non-linearity with our model, we discretized the space in front of the monkey. This allowed us to assign a beta coefficient for each spatial volume we considered and allowed to take into account both linear and non-linear gaze modulations with a unique model, approximating neural activity within each volume. First, considering that the reaching targets are in a central frontal position and the animal has to fix them for most part of the trial, we focused on this subregion of the space. We considered the position of the central nearest target as the origin of our x-y (version-elevation) coordinates system. Then we discretized the space in a 15° wide 2D grid that spanned from -22,5° (left side) up to 22,5° (right side) of version (with targets located at -15°,0°,15°) and from -22,5° (bottom) to 22,5° (up) of elevation; we divided the remaining space outside the grid in 4 quadrants (top-right, bottom-right and so on). Note that, since the targets were located at the eye level, elevation during all the fixations was ideally always 0°. For this reason, variations along the vertical coordinate happened most during the free epoch at the beginning of each trial. In addition, we created a 5° wide subdivision based on the vergence obtaining 4 layers of depth (from 20° up to 0°). This subdivision spanned from 20° of vergence (about 8-10 cm of distance from cyclopic eye) up to 0° (infinite distance, with targets located at 17°, 11°, 7°). We chose 20° as maximum limit for the vergence because no object or point of interest for the monkey was nearer than 8-10 cm. We considered each volume obtained from this double-discretization as a dummy variable that took value of 1 only when the monkey 'watches in it'. To have a reliable reference level we removed the dummy variable corresponding to the volume with coordinates (-7,5)°-7,5° (version) x (-7,5)°-7,5° (elevation) 15°-10° (vergence). In this manner we obtained 51 dummy variables ((9 squares in the 2D grid + 4 quadrants) x 4 layers of vergence – 1) indicating for each bin where the animal was looking. We considered them as the EYE POSITION block of regressors of our model.

Then, to compute x,y eye movement velocity, for each bin, for each eye, we subtracted the initial position from the final position of raw eye track , then we divided this angular variation for bin width

(40 ms) and averaged the values of the two eyes. Thus we obtained an average of gaze movement velocity in that particular bin (°/ms) (x>0, rightward movements; for y>0, upward movements). We normalized it for its highest value across all condition and all trial. In order to take into account actual saccadic neural activity, but also post- and pre-saccadic activity (Kutz et al., 2003), we built several pairs of vectors applying this procedure to eye tracks at bin t, but also to eye tracks at bin t-1, t-2 ... t+1, t+2, … t+n, spanning for the 4 previous and following bins. In this way we fed the model with information on eye movements going from -160 ms up to +160 ms around each bin. We used these vectors as the EYE SPEED/DIR block of regressors of our model.

We built other regressors to take into account the main behavioural epochs of the task. We chose the following epochs: POSTSACC (from fixation start to 500ms after it), DELAY (from target onset to go signal), PREP (from 500ms before go signal to go signal itself), PREMOV (from 200ms before home button release to home button release itself, if more than 200 ms passed after go signal; otherwise, from go signal to home button release) , MOV (from home button release to target touch), HOLD (from target touch to led colour switch), PREMOV2 (from 200ms before target release to target release itself, if more than 200 ms passed after go signal; otherwise, from led colour switch to target release), MOV2 (from target release to Home button pression).

Each of these blocks of regressors contained 9 dummy variables (1 for each target). The first dummy variable for MOV, for example, took the value of 1 in bins in which the animal was moving the arm toward first position in the space and it took 0 in all other bins; the second dummy variable, was 1 for movements toward second targets and so on. We added to the blocks of PREMOV and PREMOV2 regressors a variable containing the reaction time for each trial (normalized on the maximum across all trials and all conditions). We added to the blocks of MOV and MOV2 regressors a variable containing the average movement velocity calculated as the ratio between the distance home button-target and the movement time (normalized on the maximum across all trials and all conditions).

EYE POSITION, EYE SPEED/DIR, POSTSACC, DELAY, PREP, PREMOV, MOV, HOLD, PREMOV2, MOV2 were our blocks of extrinsic regressors.

Intrinsic regressors

We added to the model 5 independent variables providing information about spike history grouped in the block of intrinsic regressors. The first one associated each bin t to spike count at bin t-1, the second one associated each bin t to spike count at bin t-2 and so on. Past spike count had been normalized for his maximum value across all trials and all conditions. In this way, we provided to the model information about the neural activity in the previous 200 ms. In the context of GLMs, it is common to give the model information about other cells' activity in order to take into account cross correlations within the population of neurons (Truccolo et al., 2010). In our case, as our recordings were performed with single electrodes and not simultaneously, we exclude the possibility of crosstalk between neurons of our population and we did not provide any information about other cells' activity.

Fitting procedures

With data consisting on the spike count (dependent variable) and all the vectors of regressors (independent variables), for each cell independently we fitted different Generalized Linear Models following a double-step procedure. Note that our dataset consisted more than 10^4 datapoints for each cell (118 bins for each trial, 10 trials for target, 9 targets), enough to handle the $\simeq$150 variables we had with a good confidence interval.

In the first step, to make a selection of the regressors and retain only the important on cell neural activity, we fitted a GLM with all the available regressors applying the LASSO regularization. This regularization has the property to shrink the unimportant regressions coefficients to zero, so these features can be removed from the model. During this first phase, we performed a 10-fold automatic cross-validation (option 'CV' in *lassoglm* Matlab function that random datapoints to one out of 10 subsets of roughly equal size) to choose the value of λ (see equation 4) that minimizes the deviance

of the model. This step allowed us to exclude from the subsequent phase the regressors that got a regression coefficient equal to zero.

In the second step, we fitted different classic GLMs with Poisson distribution using the remaining selected features, grouped in blocks (see Extrinsic Regressors) We performed a leave-one-out cross-validation (training on 9 randomly chosen trials for each target and validating the model on the left-out 1). We repeated this cross-validation procedure 10 times for each model for each cell.

Note that each subset contained ≃9500 datapoints for training and ≃1000 points for testing. Predicted firing rate and the other statistics reported are computed on the test sets.

For each cell, we fitted several models: a "complete" one using all the regressor blocks, 10 "nested" models excluding from the complete model a different extrinsic block of regressors at a time, an "intrinsic only" model removing all the extrinsic regressor blocks, an "extrinsic only" model removing all the intrinsic regressor blocks and finally a "null" model with only the intercept that represented the ground zero goodness of fit. All the analyses and results reported in this paper were relative to these non-LASSO-regularized models.

Units selection and analysis of fitted models

Single cell level

We tried to select task-related cells to reduce noise in our population. For this purpose, we computed the mean firing rate in each epoch of interest (8, see 'Extrinsic regressors' for more details) in each trial and we performed one-way ANOVA (factor: epoch; levels: 8). All units resulted significantly modulated in at least one epoch (ANOVA $p<0.05$ for every unit). Thus, we proceeded with a cell selection based on the fitting of our model (see below).

To quantify our complete model goodness of fit and make it easy to interpret, we used a pseudo-R^2. McFadden's pseudo-R^2, for Poisson GLMs, can be calculated (Cameron and Windmeijer, 1997) starting from the log-likelihood of the complete fitted (ℓ_{complete}) and null (ℓ_{null}) models:

$$R^2_{\text{pseudo}} = 1 - \frac{\ell_{\text{complete}}}{\ell_{\text{null}}}$$

The log-likelihood of the null model (a model with only the intercept) represented the ground zero value and, by definition, it is independent from every regressor Note that McFadden's pseudo-R^2 can be interpreted as the more common R^2 in ordinary linear regression, ranging from 0 (extremely poor fit) to 1 (perfect fit), but its values tend to be considerably lower (values of 0.2 to 0.4 are considered excellent fit). When calculated on test datasets (data never seen by the model during the fitting), pseudo-R^2 values are even lower. We selected those units that reached at least a pseudo-R^2 relative to the complete model of 0.05 to discard the noisier part of population or neurons for which our model failed to capture neural activity modulations (Goodman et al., 2019; Paninski et al., 2004a).

To analyze the nested models (see 'Fitting procedures') and to get a score associated with the importance on neural activity of the information contained in every block of regressors, we proceeded as follows.

First at all, we calculated a relative pseudo-R^2 as:

$$R^2_{\text{relativepseudo}} = \frac{\ell_{\text{nested}} - \ell_{\text{null}}}{\ell_{complete} - \ell_{\text{null}}}$$

Where ℓ_{nested} is the log-likelihood of the nested model. This value compares the log-likelihood (i.e. the goodness-of-fit) of each nested model with the one of the complete model (and of the null model). Then, for an higher interpretability, we converted the relative pseudo-R^2 in a weight (w-value):= 1 - relative pseudo-R^2 .We used this as a score directly associated with the importance of groups of variables on the complete model. The idea behind this metric is that to build each nested model, we removed from the complete model a block of regressors, leading a worsening in the fitting. Whether a block of regressors contained important information for the model, its removal causes a great worsening of the fit, the relative pseudo-R^2 will decrease (towards 0) and the w-value will increase (towards 1). Vice versa, whether a regressors' block had little influence on the complete model, its removal will cause a little worsening of the fit, an increase (towards 1) in the relative pseudo-R^2 resulting finally in a little w-value (towards 0). From these computations, we obtained a set of w-

values (1 for each extrinsic block of regressors, 10 in total; 1 for the extrinsic-only model that corresponds to the removal of the SPIKE HISTORY block and 1 for the intrinsic-only model) for each selected cell that allowed us to evaluate the influence of the different parts of our model on neural activity.

It is worthy to remark that the w-values express the goodness of fit of the nested model in comparison with the complete one. Thus, a neuron can have a larger w-value for a block of regressors than another having less deviance explained by that block in absolute. Furthermore, they do not carry necessarily information about the spatial tuning of the cell. We used the 10 w-values of the extrinsic blocks to build the 'functional fingerprint' for each unit. This fingerprint shows how the cell is sensitive to the various external factors considered by our model.

Population level: extrinsic blocks of regressors

We further analyzed the extrinsic blocks of regressor across the population. We checked consistency of the results in the animals comparing the distribution of median values for all the blocks of regressors between the two animals (two-samples Kolmogorov-Smirnov test, $p<0.05$). To find the elbow of the w-values distributions (Fig. 3B), we first split the curves in two parts and then fitted one line for each part. We repeated this procedure to find the dividing point (the elbow) that minimize the sum of fitting errors.

We used PCA to reduce dimensions of data and to visualize them in a 3D space (the first 3 PCs). To look for a clustering in the population based on type of modulations (for example visual cells, motor cells, visuomotor cells modulated by gaze-position and movement, but not by hold epoch…), we then applied K-means clustering algorithm on the raw w-values (not manipulated with PCA). This algorithm needs the number of clusters to seek in input. So, to find out the optimal one, we tried with three of the most common procedures: elbow, average silhouette and Gap statistic method. Furthermore, we also tried a hierarchical clustering of the w-values. All the techniques we employed failed in finding different clusters in the data. To highlight the continuity in the modulations and the

mixed selectivity characteristic of area V6A, we coloured the dots in PCA representation according to the w-values of the three most important extrinsic blocks of regressors.

In order to study the selectivity for one of the extrinsic blocks of regressors (or the lack of it, i.e. mixed selectivity), we chose to calculate the number of important blocks on each unit spiking activity. For each cell, we summed all its extrinsic w-values. Then, we iteratively added together in descending order the extrinsic w-values up to reach 85 % of the total sum. The blocks required to achieve this value have been identified as important on that cell spiking activity. The obtained number can range from 1 (cell selective for only one feature) to 9 (cell equally selective for all the 10 features).

Spatial and temporal correlations

To study the spatial and temporal evolution of the population encoding, we performed a correlation analysis on the beta coefficients resulting from the complete models (Zhang et al. 2017). For each cell, we averaged the beta coefficients resulting from the 10 cross-validation training subsets. We then built a population vector with the beta coefficients of each cell for every spatial position and every epoch. We evaluated the correlations between vectors of beta coefficients of each pair of positions within each epoch separately (spatial correlations) and between vectors of beta coefficients of each position in subsequent epochs (temporal correlations) with the Spearman's rank correlation coefficient ($R_{Spearman}$). This coefficient does not assess linearity between the variables, but only monotonic relationships and, exploiting the rank, it is less sensitive to the outliers.

We used a linear regression to assess the dependence (r) of strength of correlations ($R_{Spearman}$) on the spatial distance between two target position (measured directly on the reaching panel, Fig. 1B).

Finally, we averaged both the spatial and the temporal correlations to have results easier to interpret.

Spike history influence

The influence of the intrinsic part of the model on the fitting has been evaluated plotting the w-values for the intrinsic part of the model and for the extrinsic part(calculated on the extrinsic-only and intrinsic-only models, respectively) in a scatterplot where each dot represents a cell. We extracted

from the complete model the 5 beta coefficients relative to different lags of the spike history for each cell and we ran on them a K-means clustering algorithm with 100 replicates with different random initial centroids and choosing the result with the lowest sum of point-to-centroid distances. We tested whether there was an association between the 2 clusters and the 2 animals with a chi-squared test (n° of M1 units in one cluster / total n° of M1 units vs n° of M2 units in the same cluster / total n° of M2 units). To represent these data, we used PCA to reduce their dimensionality projecting the cells and their clustering in the plane of the first 2 PCs. We averaged the 5 beta coefficients within each cluster and tested if distributions of the 5 beta coefficients were different between the clusters (t-test, $p<0.05$).

References

Breveglieri, R., Galletti, C., Bò, G.D., Hadjidimitrakis, K., Fattori, P., (2014). Multiple Aspects of Neural Activity during Reaching Preparation in the Medial Posterior Parietal Area V6A. J. Cogn. Neurosci. 878–895.

Breveglieri, R., Hadjidimitrakis, K., Bosco, A., Sabatini, S., Galletti, C., Fattori, P., (2012). Eye Position Encoding in Three-Dimensional Space: Integration of Version and Vergence Signals in the Medial Posterior Parietal Cortex. J. Neurosci. 32, 159–169.

Cameron, A.C., Windmeijer, F.A.G., (1997). An R-squared measure of goodness of fit for some common nonlinear regression models. J. Econom. 77, 329–342.

Dayan, P., Abbott, L.F., (2001). Theoretical Neuroscience - Computational and Mathematical Modeling of Neural Systems (The MIT Press).

Galletti, C., Fattori, P., Kutz, D.F., Gamberini, M., (1999). Brain location and visual topography of cortical area V6A in the macaque monkey. Eur. J. Neurosci. Vol. 11, 575-582.

Galletti, C., Battaglini, P.P., Fattori, P., (1995). Eye Position Influence on the Parieto-occipital Area PO (V6) of the Macaque Monkey. European Journal of Neuroscience 7(12).

Goodman, J.M., Tabot, G.A., Lee, A.S., Suresh, A.K., Rajan, A.T., Hatsopoulos, N.G., Bensmania, S., (2019). Postural Representations of the Hand in the Primate Sensorimotor Cortex Article Postural Representations of the Hand in the Primate Sensorimotor Cortex. Neuron 104, 1000-1009.e7.

Hatsopoulos, N.G., Xu, Q., Amit, Y., (2007). Encoding of Movement Fragments in the Motor Cortex. J. Neurosci. 27, 5105–5114.

Kutz, D.F., Marzocchi, N., Fattori, P., Cavalcanti, S., Galletti, C., (2005). Real-Time Supervisor System Based on Trinary Logic to Control Experiments with Behaving Animals and Humans. J. Neurophysiol. 93, 3674–3686.

Kutz, D.F., Fattori, P., Gamberini, M., Breveglieri, R., Galletti, C., (2003). Early- and late-responding cells to saccadic eye movements in the cortical area V6A of macaque monkey. Exp Brain Res 83–95.

Lehmann, S.J., Scherberger, H., (2013). Reach and gaze representations in macaque parietal and premotor grasp areas. J. Neurosci. 33, 7038–49.

Luppino, G., Ben Hamed, S., Gamberini, M., Matelli, M., Galletti, C., (2005). Occipital (V6) and parietal (V6A) areas in the anterior wall of the parieto-occipital sulcus of the macaque: A cytoarchitectonic study. Eur. J. Neurosci. 21, 3056–3076.

Paninski, L., Fellows, M.R., Hatsopoulos, N.G., and Donoghue, J.P., (2004a). Spatiotemporal tuning of motor cortical neurons for hand position and velocity. J. Neurophysiol. 91, 515–532.

Paninski, L., (2004b). Maximum likelihood estimation of cascade point-process neural encoding models. Netw. Comput. Neural Syst. 15, 243–262.Parthasarathy, A., Herikstad, R., Bong, J.H., Medina, F.S., Libedinsky, C., Yen, S.C., (2017). Mixed selectivity morphs population codes in prefrontal cortex. Nat. Neurosci. 20, 1770–1779.

Pillow, J.W., Shlens, J., Paninski, L., Sher, A., Litke, A.M., Chichilnisky, E.J., Simoncelli, E.P., (2008). Spatio-temporal correlations and visual signalling in a complete neuronal population. Nature.

Takahashi, K., Best, M.D., Huh, N., Brown, K.A., Tobaa, A.A., Hatsopoulos, N.G., (2017). Encoding of both reaching and grasping kinematics in dorsal and ventral premotor cortices. J. Neurosci. 37, 1733–1746.

Triplett, M.A., Goodhill, G.J., (2019). Probabilistic Encoding Models for Multivariate Neural Data. Front. Neural Circuits 13.

Truccolo, W., Hochberg, L.R., Donoghue, J.P., (2010). Collective dynamics in human and monkey sensorimotor cortex: Predicting single neuron spikes. Nat. Neurosci. 13, 105–111.

Truccolo, W., Eden, U.T., Fellows, M.R., Donoghue, J.P., Brown, E.N., (2005). A Point Process Framework for Relating Neural Spiking Activity to Spiking History, Neural Ensemble, and Extrinsic Covariate Effects. J. Neurophysiol. 93, 1074–1089.

Zhang, C.Y., Aflalo, T., Revechkis, B., Rosario, E.R., Ouellette, D., Pouratian, N., Andersen, R.A., (2017). Partially Mixed Selectivity in Human Posterior Parietal Association Cortex. Neuron 95, 697-708.e4.